# EXPLAINING EXTREME EVENTS OF 2014

## From A Climate Perspective

**Special Supplement to the**
***Bulletin of the American Meteorological Society***
**Vol. 96, No. 12, December 2015**

# EXPLAINING EXTREME EVENTS OF 2014 FROM A CLIMATE PERSPECTIVE

**Editors**

Stephanie C. Herring, Martin P. Hoerling, James P. Kossin, Thomas C. Peterson, and Peter A. Stott

**Special Supplement to the**

*Bulletin of the American Meteorological Society*

Vol. 96, No. 12, December 2015

**American Meteorological Society**

Corresponding Editor:

Stephanie C. Herring, PhD
NOAA National Centers for Environmental Information
325 Broadway, E/CC23, Rm 1B-131
Boulder, CO 80305-3328
E-mail: stephanie.herring@noaa.gov

Cover credits:

Front: ©iStockphotos.com/coleong—Winter snow, Boston, Massachusetts, United States.

Back: ©iStockphotos.com/nathanphoto—Legget, California, United States – August 13, 2014: CAL FIRE helicopter surveys a part of the Lodge Fire, Mendocino County.

## HOW TO CITE THIS DOCUMENT

Citing the complete report:

Herring, S. C., M. P. Hoerling, J. P. Kossin, T. C. Peterson, and P. A. Stott, Eds., 2015: Explaining Extreme Events of 2014 from a Climate Perspective. *Bull. Amer. Meteor. Soc.*, **96** (12), S1–S172.

Citing a section (example):

Yoon, J. H., S.-Y. S. Wang, R. R. Gillies, L. Hipps, B. Kravitz, and P. J. Rasch, 2015: Extreme fire season in California: A glimpse into the future? [in "Explaining Extremes of 2014 from a Climate Perspective"]. *Bull. Amer. Meteor. Soc.*, **96** (12), S5–S9.

## EDITORIAL AND PRODUCTION TEAM

**Riddle, Deborah B.,** Lead Graphics Production, NOAA/NESDIS National Centers for Environmental Information, Asheville, NC

**Love-Brotak, S. Elizabeth,** Graphics Support, NOAA/NESDIS National Centers for Environmental Information, Asheville, NC

**Veasey, Sara W.,** Visual Communications Team Lead, NOAA/NESDIS National Centers for Environmental Information, Asheville, NC

**Griffin, Jessicca,** Graphics Support, Cooperative Institute for Climate and Satellites-NC, North Carolina State University, Asheville, NC

**Maycock, Tom,** Editorial Support, Cooperative Institute for Climate and Satellites-NC, North Carolina State University, Asheville, NC

**Misch, Deborah J.,** Graphics Support, LMI Consulting, Inc., NOAA/NESDIS National Centers for Environmental Information, Asheville, NC

**Osborne, Susan,** Editorial Support, LMI Consulting, Inc., NOAA/NESDIS National Centers for Environmental Information, Asheville, NC

**Schreck, Carl,** Editorial Support, Cooperative Institute for Climate and Satellites-NC, North Carolina State University, and NOAA/NESDIS National Centers for Environmental Information, Asheville, NC

**Sprain, Mara,** Editorial Support, LAC Group, NOAA/NESDIS National Centers for Environmental Information, Asheville, NC

**Young, Teresa,** Graphics Support, STG, Inc., NOAA/NESDIS National Centers for Environmental Information, Asheville, NC

# TABLE OF CONTENTS

**ABSTRACT—**Stephanie C. Herring, Martin P. Hoerling, James P. Kossin, Thomas C. Peterson, and Peter A. Stott

Understanding how long-term global change affects the intensity and likelihood of extreme weather events is a frontier science challenge. This fourth edition of explaining extreme events of the previous year (2014) from a climate perspective is the most extensive yet with 33 different research groups exploring the causes of 29 different events that occurred in 2014. A number of this year's studies indicate that human-caused climate change greatly increased the likelihood and intensity for extreme heat waves in 2014 over various regions. For other types of extreme events, such as droughts, heavy rains, and winter storms, a climate change influence was found in some instances and not in others. This year's report also included many different types of extreme events. The tropical cyclones that impacted Hawaii were made more likely due to human-caused climate change. Climate change also decreased the Antarctic sea ice extent in 2014 and increased the strength and likelihood of high sea surface temperatures in both the Atlantic and Pacific Oceans. For western U.S. wildfires, no link to the individual events in 2014 could be detected, but the overall probability of western U.S. wildfires has increased due to human impacts on the climate.

Challenges that attribution assessments face include the often limited observational record and inability of models to reproduce some extreme events well. In general, when attribution assessments fail to find anthropogenic signals this alone does not prove anthropogenic climate change did not influence the event. The failure to find a human fingerprint could be due to insufficient data or poor models and not the absence of anthropogenic effects.

This year researchers also considered other human-caused drivers of extreme events beyond the usual radiative drivers. For example, flooding in the Canadian prairies was found to be more likely because of human land-use changes that affect drainage mechanisms. Similarly, the Jakarta floods may have been compounded by land-use change via urban development and associated land subsidence. These types of mechanical factors re-emphasize the various pathways beyond climate change by which human activity can increase regional risk of extreme events.

# 16. ASSESSING THE CONTRIBUTIONS OF EAST AFRICAN AND WEST PACIFIC WARMING TO THE 2014 BOREAL SPRING EAST AFRICAN DROUGHT

Chris Funk, Shraddhanand Shukla, Andy Hoell, and Ben Livneh

*Anthropogenic warming contributed to the 2014 East African drought by increasing East African and west Pacific temperatures, and increasing the gradient between standardized western and central Pacific SST causing reduced rainfall, evapotranspiration, and soil moisture.*

*Introduction.* During April–June of 2014 some areas of East Africa (EA) experienced substantial rainfall deficits (Funk et al. 2014) and warm land surface temperatures (Supplemental Fig. S16.1). Here, using the Variable Infiltration Capacity model (VIC; Liang et al. 1994; Nijssen et al. 1997), we evaluate and contrast the potential influence of (i) warm East African air temperatures and (ii) rainfall reductions associated with a more intense West Pacific Index (WPI; Funk et al. 2014). The WPI is a standardized version of the West Pacific Gradient (Hoell and Funk 2013a); here defined as the standardized difference between the Niño 4 and West Pacific (WP; 10°S–10°N, 110°–150°E) SST (Funk et al. 2014): WPI = Z(Z(Niño 4) − Z(WP)), where Z() denotes standardization.

The April–June 2014 drought, like many droughts over the past 20 years, occurred in conjunction with an enhanced WP SST gradient (Funk et al. 2014; Liebmann et al. 2014; Lyon and DeWitt 2012; Shukla et al. 2014a). Interagency research by Famine Early Warning Systems Networks (FEWS NET) scientists has been focusing on using SST gradients to predict some of these spring droughts (Funk et al. 2014; Shukla et al. 2014a; Shukla et al. 2014b). Climate model ensembles reveal strong 3-month lagged WPI–EA spring rainfall relationships (Funk et al. 2014), and these simulation results help justify successful forecasts based on empirical relationships (Funk et al. 2014) or hybrid statistical–dynamic forecasts (Shukla et al. 2014a). Diagnostic analyses of simulations from the ECHAM5 (Liebmann et al. 2014) and GFSv2 (Hoell and Funk 2013b) models help confirm these relationships, and WP SST gradients were used to predict the 2014 boreal spring drought (Funk et al. 2014). Extreme WPI conditions represent a combination of warming west Pacific SST (Funk and Hoell 2015) and La Niña-like cool central Pacific SST, which enhances rainfall and moisture convergence over the Indo-Pacific warm pool while decreasing it over eastern East Africa (Hoell and Funk 2013b; Hoell et al. 2014; Liebmann et al. 2014; Williams and Funk 2011).

*Methods and Results.* While 2014 EA air temperatures and WP SST anomalies were extremely warm, Niño 4 SST anomalies were not. Figures 16.1a–c compare the observed EA air temperatures, WP and Niño 4 SST to 1900–50 probability density functions (PDFs) based on observations, and an ensemble of historical (Taylor et al. 2011) simulations based on all forcings (natural and anthropogenic) from the Coupled Model Intercomparison Project Phase 5 (CMIP5; Supplemental Table 16.1). The selected EA region (Supplemental Fig. S16.1) was chosen because it was hot and dry in 2014, and reasonably homogeneous (Funk et al. 2014). The +1°C NASA Goddard Institute for Space Studies (GISS) air temperature anomaly (Hansen et al. 2010) far exceeds the 1900–50 PDFs based on historical observations or the CMIP5 historical simulations. The 1900–50 period was used to represent near preindustrial conditions. When bias corrected using the ratio of the observed (0.53°C) and simulated (0.42°C) temperatures, the smoothed (15-yr average) CMIP5 ensemble mean tracks very closely with observations (r = 0.97; Fig. 16.1d), and the observed +1°C anomaly is very similar to the center of the 2014 CMIP5 PDF (Fig. 16.1a) and the mean of the CMIP5 ensemble (0.99°C). Thus, we find that (i) the CMIP5 models do a very good job of recreating

Affiliations: Funk—U.S. Geological Survey, and University of California, Santa Barbara, Santa Barbara, California; Shukla—University of California, Santa Barbara, Santa Barbara, California; Hoell—NOAA, Earth System Research Laboratory Physical Sciences Division, Boulder, Colorado; Livneh—Department of Civil, Environmental, and Architectural Engineering & Cooperative Institute for Research in Environmental Sciences, University of Colorado, Boulder, Colorado

DOI: 10.1175/BAMS-D-15-00106.1

A supplement to this article is available online (10.1175/BAMS-D-15-00106.2)

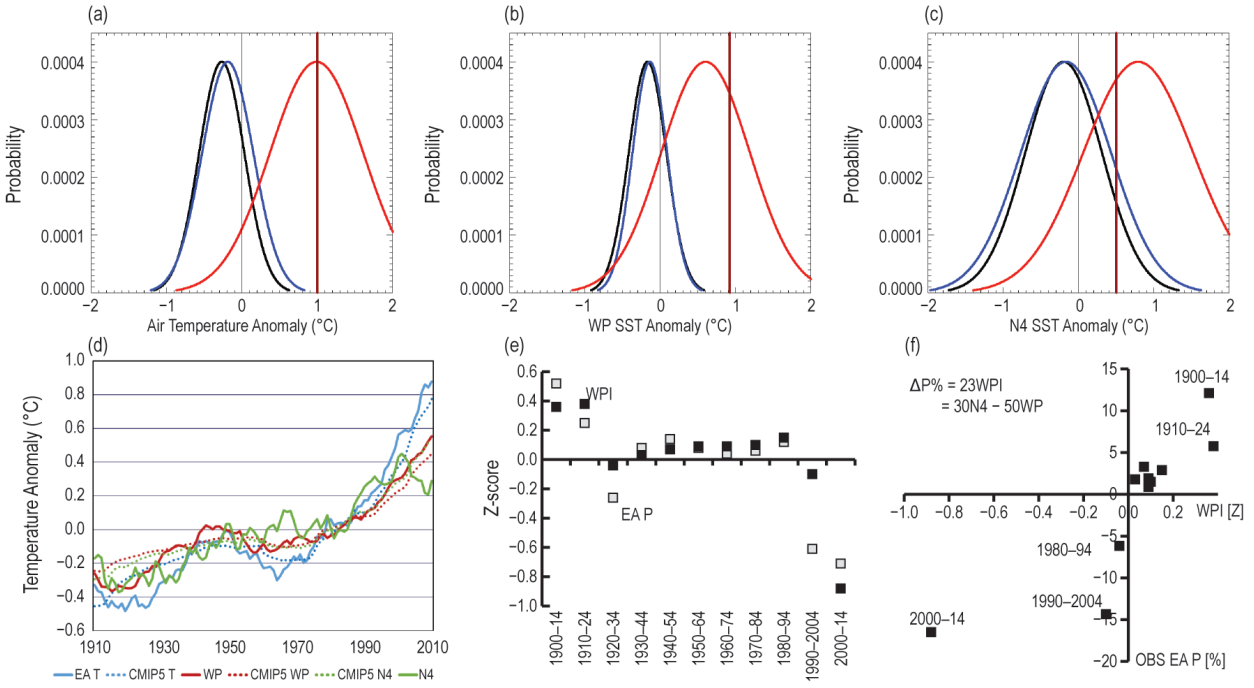


**Fig. 16.1. (a) East African air temperature anomalies PDFs based on 1900–50 observations (black), 1900–50 CMIP5 simulations (blue), and 2014 CMIP5 all forcings (natural and anthropogenic) simulations (red); observed 2014 air temperatures shown with a vertical line. (b) As in (a) but for WP SSTs. (c) As in (a) but for Niño 4 SSTs. (d) Observed and CMIP5 time series, smoothed with 15-yr running means. (e) 15-yr averages of the WPI and standardized EA precipitation. (f) Same data as a scatterplot. All data are expressed as anomalies from a 1900–2014 reference period.**

the observed pattern of warming (Fig. 16.1d), (ii) the observed +1°C anomaly appears extremely unlikely without recent anthropogenic warming, and (iii) the observed +1°C warming was very likely to be due in part to anthropogenic influences.

We find similar results when examining WP SSTs (Fig. 16.1b). The large +0.9 WP SST anomaly—the warmest in the extended reconstruction dataset (Smith et al. 2008)—sits far beyond the observed and historical CMIP5 1900–50 PDFs. WP SST is heavily influenced by radiative forcing (Funk and Hoell 2015) and tracks closely with the CMIP5 ensemble mean ($r = 0.96$; Fig. 16.1d). The observed +0.9°C anomaly is substantially more than the CMIP5 prediction (+0.6°C). Here again, we find that (i) the CMIP5 models do a very good job of recreating the observed pattern of warming (Fig. 16.1d), (ii) the observed +0.9°C anomaly appears extremely unlikely without recent anthropogenic warming, and (iii) the observed +0.9°C warming was very likely to be due in part to anthropogenic influences.

Niño 4 SSTs have high interannual variance, and the chances of an anomaly as warm as or warmer than the observed +0.5°C anomaly occurring were therefore likely (Fig. 16.1c) given the variance in both the observed and CMIP5 1900–50 PDFs (8% and 13%, respectively; Table 16.1). Between 1900 and 1990, the observed Niño 4 time series tended to follow the CMIP5 mean (Fig. 16.1d), but since about 1990, warming in the Niño 4 region has been limited (Funk et al. 2014). This relative cooling may be due to Pacific Decadal Variability (PDV; Lyon et al. 2013; Meehl et al. 2013) or perhaps a poorly understood and poorly forced response, which might potentially be related to increased warm pool SSTs, precipitation, and more rapid central Pacific trade winds (Funk and Hoell 2015). The observed 2000–14 Niño 4 average (0.28°C) was substantially below the +0.5°C warming predicted by the CMIP5 simulations (Fig. 16.1d).

Figures 16.1e and f show 1900–2014 EA Centennial Trends (CenTrends; Funk et al. 2015) precipitation as a function of the WPI. These data are from the new FEWS NET CenTrends archive (Funk et al. 2015). CenTrends incorporate numerous stations from the Nicholson database (Nicholson et al. 2012) and observations acquired from the Tanzanian, Kenyan, and Ethiopian Meteorological Agencies (Funk et al. 2015). Decadal CenTrends (Funk et al. 2015) and the Global Precipitation Climatology Centre dataset (Funk et al. 2014) EA spring rainfall vary with WP/Niño SST

**Table 16.1. Observed and modeled anomalies. Probabilities with and without climate change were based, respectively, on the 2014 and the 1900–50 values from the CMIP5 ensemble (Supplemental Table S16.1).**

| Observation | Observation anomaly | 1900–2014 Percentile Observation (CMIP5) | Probability 1900–1950 PDF Observation (CMIP5) | Probability 2014 PDF | Estimated anthropogenic contribution |
|---|---|---|---|---|---|
| **AMJ air temperatures** | +1.0°C† | 96.5% (97.9%) | 0% (0%) | (50%) | +1.0°C |
| **WP SST** | +0.9°C† | 100% (99.6%) | 0% (0%) | (30%) | +0.6°C |
| **Niño 4 SST** | +0.5°C | 82% (78%) | 8% (13%) | (66%) | +0.6°C |
| **Z(N4) - Z(WP)** | −1.9°C | 16% (0%) | 8% (0%) | (1%) | −0.6°C |
| **AMJ CenTrends P** | −0.8σ† | | | | −0.4σ* |
| **AMJ ET** | −1σ‡ | | | | −0.σ** 0.0σ *** |
| **AMJ soil moisture** | −0.5σ‡ | | | | −0.3σ** 0.0σ*** |

† Based on 1900–2014 baseline

‡ Based on 1982–2014 baseline

* Based on estimated anthropogenic contribution to WP warming and the WPI regression results shown in Fig.16.1f.

** Based on assumed 11% WP-related rainfall reduction and +1°C anthropogenic warming.

*** Based on an assumed +1°C anthropogenic warming.

gradients (Fig. 16.1e), falling markedly during the 1990s and 2000s as the WP warmed and the Niño 4 did not (Fig. 16.1d). ECHAM5 (Liebmann et al. 2014) and GFSv2 (Funk et al. 2014) and CESM (Funk et al. 2014) models help confirm the WPI–EA relationship (Supplemental Fig. S16.2).

The data shown in Fig. 16.1f imply a quasi-linear relation with the percent change EA April–June rainfall equal to 23 times the WPI. By inverting the WPI standardization: Z(Z(N4) − Z(WP)), we can estimate changes based on SST anomalies: ΔP% = 30Niño 4 − 49WP. While the observed WP warming has been substantially greater than Niño 4 warming (Fig. 16.1d) and the 2014 WP values the warmest on record (+0.9°C; Fig. 16.1b), here we simply test the impact associated with an identical +0.6°C "bathtub" anthropogenic warming in each region. Under this assumption, rainfall would decrease by 11%; ΔP% = 30 • 0.6 − 49WP • 0.6 = −11%.

We next assess the possible hydrologic impacts associated with an assumed +1°C increase in EA air temperatures, based on the CMIP5 ensemble mean, and an 11% rainfall decrease using the VIC model (Liang et al. 1994; Nijssen et al. 1997), which has been used to analyze recent EA drought (Sheffield et al. 2014; Shukla et al. 2014b). We evaluate these impacts by contrasting VIC simulations forced with the observed 2014 precipitation and temperatures (Supplemental Fig. S16.3) with (i) simulations forced with 11% more precipitation and 1°C cooler air temperatures and (ii) simulations forced with observed precipitation and 1°C cooler air temperatures (Figs. 16.2b,c).

We begin by showing recent changes in April–June hydrology (Fig. 16.2a). The well-documented post-1999 decline (Funk and Hoell 2015; Funk et al. 2014; Hoell and Funk 2013b; Liebmann et al. 2014; Lyon 2014; Lyon and DeWitt 2012; Yang et al. 2014) has resulted in a 10 to 30% reduction in rainfall. Dry and warm conditions have been much more likely since 1998 across the eastern portions of EA. The associated evapotranspiration (ET) reductions follow rainfall deficits closely, and southeastern Kenya, south-central

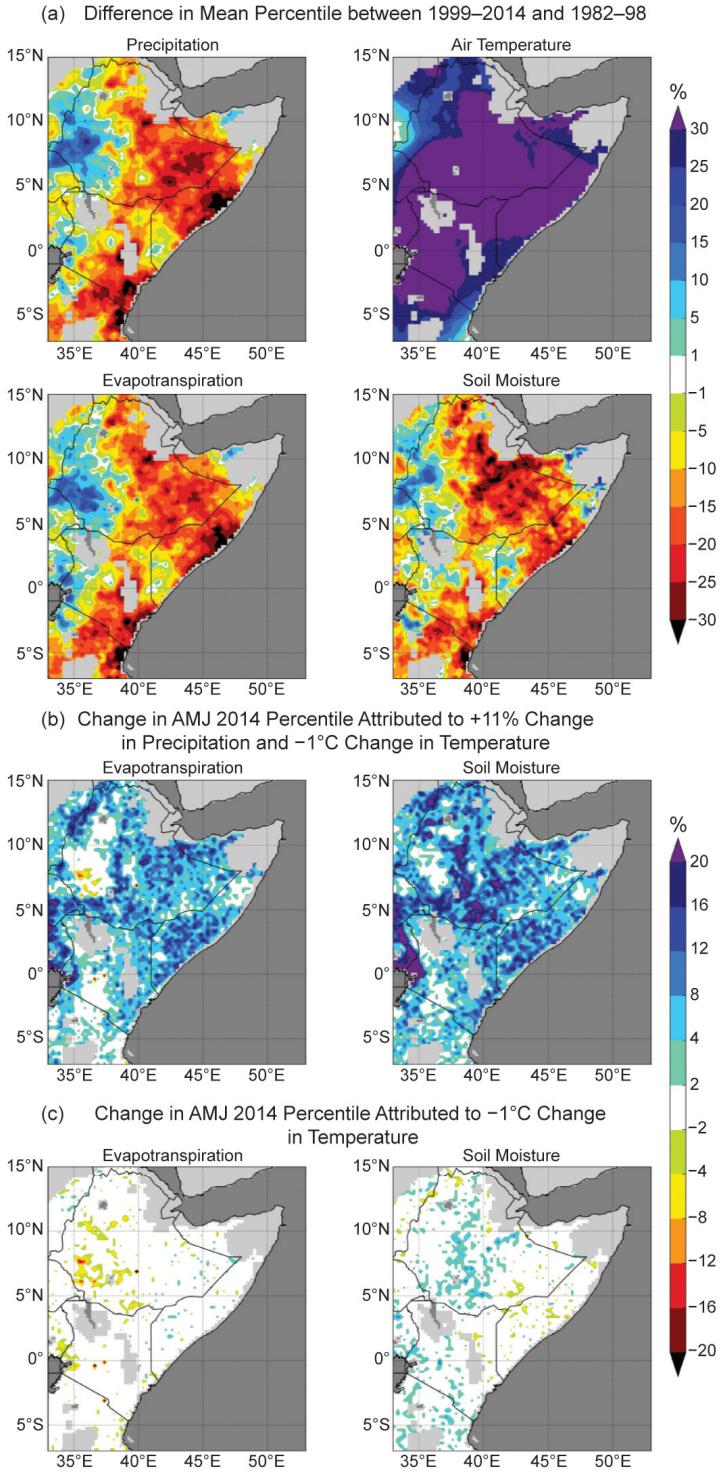


**Fig. 16.2. (a) Changes in Apr–Jun precipitation, air temperature, ET, and soil moisture between 1999–2014 and 1982–98, expressed as differences in the 1981–2014 percentiles. (b) Change in Apr–Jun 2014 ET and soil moisture percentiles, based on an 11% rainfall increase and a 1°C cooling of air temperatures. (c) As in (b) but based on just a 1°C cooling of air temperatures. Areas receiving, on average, less than 75 mm of rainfall have been masked.**

Somalia, and eastern Ethiopia appear to be the most affected.

We next compare the impact of (i) less rainfall and warmer air temperatures, and (ii) only warmer air temperatures, by using counterfactual experiments. In the first experiment (i), we increased the April–June precipitation by 11% (+0.4 standardized deviations) and reduced the air temperature by 1°C. Supplemental Fig. S16.3 compares 2014 to 2011, 2012, and 2013. While not as dry as 2011, the VIC simulations (Fig. 16.2b) indicate that much of Kenya, Somalia, and Ethiopia experienced low ET and soil moisture, with percentile values of less than 30%. The combination of increased precipitation and reduced air temperatures increased the simulated percentiles by about 4%–25% (Fig. 16.2b). In western Kenya, however, large changes in soil moisture are found in key crop producing areas of the Rift Valley. This is true as well in central Ethiopia, between 7°–10°N at about 38°E.

Figure 16.2c shows results for our experiment (ii), where we changed only the air temperatures. These results imply that, given the observed precipitation conditions, warmer air temperatures acting alone had little influence on ET and soil moisture. This may indicate that the evaporative demand, even in the −1°C scenario, was more than the available moisture supply in most places.

We can compare the 2014 anomalies to the empirical 1982–2014 distributions of ET and soil moisture, averaged over the study site (Supplemental Fig. 4). The 2014 ET anomaly was low compared to the historical distribution (a −1 standardized anomaly). Cooling the air temperatures changed this value very little. Increasing rainfall and cooling air temperatures moderated the drought, resulting in a −0.7 standardized anomaly. The 2014 soil moisture anomaly was mild (a −0.5 standardized anomaly); increasing rainfall and cooling air temperatures moderated soil moisture deficits, resulting in a −0.2 standardized anomaly. Averaging these soil moisture results across the entire domain may mask important localized impacts (Fig. 16.2b).

*Conclusion*. In summary, we found that the CMIP5 models predicted very well ($r \approx 0.96$) low frequency EA and WP temperature variations, and the very warm ~+1°C WP and EA anomalies appear extremely unlikely without anthropogenic warming. WP SSTs track closely with climate change projections (Supplemental Fig. S16.5a), climate change simulations indicate an increase in the standardized west Pacific SST gradient (Supplemental Figs. S16.5b; Fig. S16.6a), and 1900–2014 15-yr running averages of March–June Greater Horn of Africa rainfall follow closely changes in the WPI (Funk et al. 2014; Supplemental Fig. S16.5d). The Pacific SST gradient is amplified when the ENSO-related SST component is removed (Supplemental Fig. S16.6b), suggesting that stronger gradient events may occur when ENSO conditions are neutral or La Niña-like. Our hydrologic modeling results suggest that a 1°C temperature increase combined with an 11% WPI-related precipitation decrease, associated with a ~+0.6°C warming in both the WP and Niño 4 regions, would have appreciably increased the 2014 April–June drought intensity, enhancing ET and soil moisture anomalies from −0.7 and −0.2 standardized deviations to −1 and −0.5 in areas experiencing some isolated food security crises (Supplemental Fig. S16.7). Air temperature changes alone were found to have little effect.

**ACKNOWLEDGEMENTS.** This work was supported by US Geological Survey (USGS) cooperative agreement #G09AC000001), NOAA Award NA11OAR4310151, the USGS Climate and Land Use Change program, NASA SERVIR, and NASA grants NNH12ZDA001N-IDS and NNX14AD30G. We would like to thank our editor (Stephanie Herring), our anonymous reviewers, and Colin Kelley whose suggestions substantially improved this manuscript.

## REFERENCES

Funk, C., and A. Hoell, 2015: The leading mode of observed and CMIP5 ENSO-residual sea surface temperatures and associated changes in Indo-Pacific climate. *J. Climate*, **28**, 4309–4329, doi:10.1175/JCLI-D-14-00334.1.

——,——, S. Shukla, I. Bladé, B. Liebmann, J. B. Roberts, and G. Husak, 2014: Predicting East African spring droughts using Pacific and Indian Ocean sea surface temperature indices. *Hydrol. Earth Syst. Sci.*, **18**, 4965–4978, doi:10.5194/hess-18-4965-2014.

——, S. Nicholson, M. Landsfeld, D. L. Klotter, M., P. Peterson, and L. Harrison, 2015: The Centennial Trends Greater Horn of Africa precipitation dataset. *Nat. Scientific Data*, **2**, Article 150050, doi:10.1038/sdata.2015.50.

Hansen, J., R. Ruedy, M. Sato, and K. Lo, 2010: Global surface temperature change. *Rev. Geophys.*, **48**, RG4004, doi:10.1029/2010RG000345.

Hoell, A., and C. Funk, 2013a: The ENSO-related west Pacific sea surface temperature gradient. *J. Climate*, **26**, 9545–9562, doi:10.1175/JCLI-D-12-00344.1.

——, and ——, 2013b: Indo-Pacific sea surface temperature influences on failed consecutive rainy seasons over eastern Africa. *Climate Dyn.*, **43**, 1645–1660, doi:10.1007/s00382-013-1991-6.

——, ——, and M. Barlow, 2014: La Niña diversity and northwest Indian Ocean rim teleconnections. *Climate Dyn.*, **43**, 2707–2724, doi:10.1007/s00382-014-2083-y.

Liang, X., D. P. Lettenmaier, E. F. Wood, and S. J. Burges, 1994: A simple hydrologically based model of land surface water and energy fluxes for general circulation models. *J. Geophys. Res.*, **99**, 14415–14428, doi:10.1029/94JD00483.

Liebmann, B., and Coauthors, 2014: Understanding recent eastern Horn of Africa rainfall variability and change. *J. Climate*, **27**, 8630–8645, doi:10.1175/JCLI-D-13-00714.1.

Lyon, B., 2014: Seasonal drought in the Greater Horn of Africa and its recent increase during the March–May long rains. *J. Climate*, **27**, 7953–7975, doi:10.1175/JCLI-D-13-00459.1.

——, and D. G. DeWitt, 2012: A recent and abrupt decline in the East African long rains. *Geophys. Res. Lett.*, **39**, L02702, doi:10.1029/2011GL050337.

——, A. G. Barnston, and D. G. DeWitt, 2013: Tropical pacific forcing of a 1998–1999 climate shift: Observational analysis and climate model results for the boreal spring season. *Climate Dyn.*, **43**, 893–909, doi:10.1007/s00382-013-1891-9.

Meehl, G. A., A. Hu, J. M. Arblaster, J. Fasullo, and K. E. Trenberth, 2013: Externally forced and internally generated decadal climate variability associated with the interdecadal Pacific oscillation. *J. Climate*, **26**, 7298–7310, doi:10.1175/JCLI-D-12-00548.1.

Nicholson, S. E., A. K. Dezfuli, and D. Klotter, 2012: A two-century precipitation dataset for the continent of Africa. *Bull. Amer. Meteor. Soc.*, **93**, 1219–1231, doi:10.1175/BAMS-D-11-00212.1.

Nijssen, B., D. P. Lettenmaier, X. Liang, S. W. Wetzel, and E. F. Wood, 1997: Streamflow simulation for continental-scale river basins. *Water Resour. Res.*, **33**, 711–724.

Sheffield, J., and Coauthors, 2014: A drought monitoring and forecasting system for sub-Sahara African water resources and food security. *Bull. Amer. Meteor. Soc.*, **95**, 861–882, doi:10.1175/BAMS-D-12-00124.1.

Shukla, S., C. Funk, and A. Hoell, 2014a: Using constructed analogs to improve the skill of National Multi-Model Ensemble March–April–May precipitation forecasts in equatorial East Africa. *Environ. Res. Lett.*, **9**, 094009, doi:10.1088/1748-9326/9/9/094009.

——, A. McNally, G. Husak, and C. Funk, 2014b: A seasonal agricultural drought forecast system for food-insecure regions of East Africa. *Hydrol. Earth Syst. Sci.*, **18**, 3907–3921, doi:10.5194/hess-18-3907-2014.

Smith, T. M., R. W. Reynolds, T. C. Peterson, and J. Lawrimore, 2008: Improvements to NOAA's Historical Merged Land–Ocean Surface Temperature Analysis (1880–2006). *J. Climate*, **21**, 2283–2296.

Taylor, K. E., R. J. Stouffer, and G. A. Meehl, 2011: An overview of CMIP5 and the experiment design. *Bull. Amer. Meteor. Soc.*, **93**, 485–498, doi:10.1175/BAMS-D-11-00094.1.

Williams, P., and C. Funk, 2011: A westward extension of the warm pool leads to a westward extension of the Walker circulation, drying eastern Africa. *Climate Dyn.*, **37**, 2417–2435.

Yang, W., R. Seager, M. A. Cane, and B. Lyon, 2014: The East African long rains in observations and models. *J. Climate*, **27**, 7185–7202, doi:10.1175/JCLI-D-13-00447.1.

## Table 34.1. ANTHROPOGENIC INFLUENCE

### ON EVENT STRENGTH †

| | INCREASE | DECREASE | NOT FOUND OR UNCERTAIN |
|---|---|---|---|
| **Heat** | **Australia** (Ch. 31)<br>**Europe** (Ch.13)<br>**S. Korea** (Ch. 19) | | **Australia, Adelaide & Melbourne** (Ch. 29)<br>**Australia, Brisbane** (Ch.28) |
| **Cold** | | **Upper Midwest** (Ch.3) | |
| **Winter Storms and Snow** | | | **Eastern U.S.** (Ch. 4)<br>**N. America** (Ch. 6)<br>**N. Atlantic** (Ch. 7) |
| **Heavy Precipitation** | **Canada**** (Ch. 5) | | **Jakarta****** (Ch. 26)<br>**United Kingdom***** (Ch. 10)<br>**New Zealand** (Ch. 27) |
| **Drought** | **E. Africa** (Ch. 16)<br>**E. Africa*** (Ch. 17)<br>**S. Levant** (Ch. 14) | | **Middle East and S.W. Asia** (Ch. 15)<br>**N.E. Asia** (Ch. 21)<br>**Singapore** (Ch. 25) |
| **Tropical Cyclones** | | | **Gonzalo** (Ch. 11)<br>**W. Pacific** (Ch. 24) |
| **Wildfires** | | | **California** (Ch. 2) |
| **Sea Surface Temperature** | **W. Tropical & N.E. Pacific** (Ch. 20)<br>**N.W. Atlantic & N.E. Pacific** (Ch. 13) | | |
| **Sea Level Pressure** | **S. Australia** (Ch. 32) | | |
| **Sea Ice Extent** | | | **Antarctica** (Ch. 33) |

† Papers that did not investigate strength are not listed.

†† Papers that did not investigate likelihood are not listed.

* No influence on the likelihood of low rainfall, but human influences did result in higher temperatures and increased net incoming radiation at the surface over the region most affected by the drought.

** An increase in spring rainfall as well as extensive artificial pond drainage increased the risk of more frequent severe floods from the enhanced rainfall.

*** Evidence for human influence was found for greater risk of UK extreme rainfall during winter 2013/14 with time scales of 10 days

**** The study of Jakarta rainfall event of 2014 found a statistically significant increase in the probability of such rains over the last 115 years, though the study did not establish a cause.

| | ON EVENT LIKELIHOOD †† | | | Total Number of Papers |
|---|---|---|---|---|
| | INCREASE | DECREASE | NOT FOUND OR UNCERTAIN | |
| **Heat** | **Argentina** (Ch. 9)<br>**Australia** (Ch. 30, Ch. 31)<br>**Australia, Adelaide** (Ch. 29)<br>**Australia, Brisbane** (Ch. 28)<br>**Europe** (Ch. 13)<br>**S. Korea** (Ch. 19)<br>**China** (Ch. 22) | | **Melbourne, Australia** (Ch. 29) | 7 |
| **Cold** | | **Upper Midwest** (Ch.3) | | 1 |
| **Winter Storms and Snow** | **Nepal** (Ch. 18) | | **Eastern U.S.**(Ch. 4)<br>**N. America** (Ch. 6)<br>**N. Atlantic** (Ch. 7) | 4 |
| **Heavy Precipitation** | **Canada**** (Ch. 5)<br>**New Zealand** (Ch. 27) | | **Jakarta**** (Ch. 26)<br>**United Kingdom***** (Ch. 10)<br>**S. France** (Ch. 12) | 5 |
| **Drought** | **E. Africa** (Ch. 16)<br>**S. Levant** (Ch. 14) | | **Middle East and S.W. Asia** (Ch. 15)<br>**E. Africa*** (Ch. 17)<br>**N.E. Asia** (Ch. 21)<br>**S. E. Brazil** (Ch. 8)<br>**Singapore** (Ch. 25) | 7 |
| **Tropical Cyclones** | **Hawaii** (Ch. 23) | | **Gonzalo** (Ch. 11)<br>**W. Pacific** (Ch. 24) | 3 |
| **Wildfires** | **California** (Ch. 2) | | | 1 |
| **Sea Surface Temperature** | **W. Tropical & N.E. Pacific** (Ch. 20)<br>**N.W. Atlantic & N.E. Pacific** (Ch. 13) | | | 2 |
| **Sea Level Pressure** | **S. Australia** (Ch. 32) | | | 1 |
| **Sea Ice Extent** | | | **Antarctica** (Ch. 33) | 1 |
| | | | **TOTAL** | 32 |

† Papers that did not investigate strength are not listed.

†† Papers that did not investigate likelihood are not listed.

* No influence on the likelihood of low rainfall, but human influences did result in higher temperatures and increased net incoming radiation at the surface over the region most affected by the drought.

** An increase in spring rainfall as well as extensive artificial pond drainage increased the risk of more frequent severe floods from the enhanced rainfall.

*** Evidence for human influence was found for greater risk of UK extreme rainfall during winter 2013/14 with time scales of 10 days

**** The study of Jakarta rainfall event of 2014 found a statistically significant increase in the probability of such rains over the last 115 years, though the study did not establish a cause.